2021 IEEE/SICE International Symposium on System Integrations (SII)
Iwaki, Fukushima, Japan. January 11 - 14, 2021

Kinematic gait stability index highly correlated with the margin of stability: Concept and interim report

Tomoyuki Iwasaki, Shogo Okamoto, Yasuhiro Akiyama, Takashi Inagaki, and Yoji Yamada

Abstract— **Gait stability indices that are easy to measure and compute are necessary to enhance their commercial applications. We constructed a new kinematic gait variability index that is highly correlated with a popular kinetic stability index, i.e., the margin of stability (MoS). The new stability index was computed by using the velocity of the center of the human body mass, which can be easily measured by equipment such as inertial measurement instruments. A time-series extension of partial least squares regression was applied on the velocity series to construct the principal motions. These motions were independent of each other and were correlated with MoS. The linear combination of these principal motions exhibited a high correlation coefficient of 0.82 with the minimum values of MoS, suggesting that the proposed index can be used as an easy-to-measure alternative of the MoS.**

I. INTRODUCTION

Falling down while walking is a major concern for the elderly. Thus far, many studies on gait stability and stable walking have been conducted. For example, a previous study found that the stability of gait depends on some gait parameters such as the gait speed [1], [2] and step length [3], [4]. Some studies focused on how humans avoid falling after tripping or coming in contact with obstacles [5], [6]. In particular, indices to represent gait stability are invaluable for judging the risk of falling and for enhancing commercial applications such as walking aids [7].

There are two types of gait stability indices: kinetic and kinematic. Kinetic indices are computed based on the law of physical dynamics, and they directly represent the risk or safety margin of falls; however, their computation requires the measurement of the positions or angles of multiple human body parts. Further, some indices require the measurement of ground reaction forces. Hence, kinetic indices are suitable for laboratory environments. The margin of stability (MoS) [8] is a representative kinetic gait stability index. In contrast, kinematic indices are usually computed by using kinematic information of fewer body parts. Such information can be easily acquired through inertial measurements. Further, because they do not require the measurement of forces, the kinematic stability indices are relatively easy to obtain; however, they may not be directly related to kinetic stability. For example, the maximum Lyapnov exponent [9] is often used.

Considering these properties of the two types of stability indices, many studies have compared them. For example, Hak et al. compared the short-term Lyapunov exponents with the minimum MoS values in the forward direction and the medio-lateral direction and reported that they exhibit different properties [4], [10]. Vieira et al. compared the short-term Lyapunov exponents in the three axial directions with the minimum MoS values in the forward and medio-lateral directions during the walking of fatigued people. They found no substantial correlation among them [11]. Yang et al. compared the feasible stability region with the minimum MoS values, Floquet multiplier, and Lyapunov exponent for the fall prediction and concluded that they exhibited different properties [12].

One of their goals was to find kinematic stability indices that are correlated with the kinetic stability indices. If this correlation can be found, the kinetic stability indices can be replaced with easy-to-access kinematic ones. This is beneficial especially for commercial applications. However, as mentioned above, earlier studies have suggested that there is no substantial correlation between popular kinetic and kinematic stability indices. In the present study, we employ an approach that is different from those of previous studies. We construct a new kinematic index that is correlated with a popular kinetic index.

In this work, we construct a new kinematic gait variability index that is highly correlated with a popular kinetic stability index i.e., the MoS. For this, we extend partial least squares regression (PLS) [13], which is a supervised multivariate analysis, and apply it to a subset of the gait motion database [14], which is measured by a camera-based motion capture system. This kinematic index uses the time-series of velocity at the center of human body mass that can be easily measured by an inertial measurement instrument such as the one built-in phones.

II. GAIT STABILITY INDEX: MARGIN OF STABILITY

In this study, we evaluate the MoS values of participants by using the extrapolated center of mass (XCoM) [8]. For this computation, as shown in Fig. 1, the human body was approximated to be an inverted pendulum with a constant length of l. The y-axis is the forward direction, and the z-axis is the upward direction. The coordinate vector of XCoM ($\boldsymbol{x}_{com}$) was computed by the velocity vector of the center of mass (CoM) ($\boldsymbol{v}_{com}$), and it represents the range of the CoM movement at each instant. MoS is the distance vector between the XCoM and the end of the base of support (BoS). The larger the MoS value, the greater the margin against falls, because falls are induced when the CoM is outside the end of BoS. When the MoS value is negative, a human falls

*This work was in part supported by AMED (Japan Agency for Medical Research and Development 19he2002003h0302) and JSPS KAKENHI (19K21584).

All are with the Department of Mechanical Systems Engineering, Nagoya University, Nagoya, Japan.

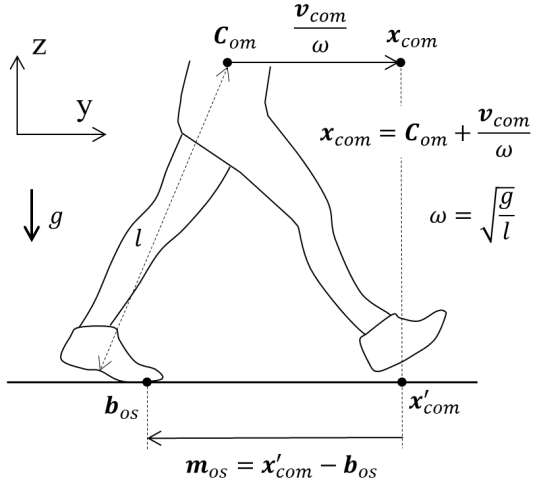

Fig. 1. Definition of MoS along the y-axis. $\boldsymbol{x}'_{com}$ is the projection of $\boldsymbol{x}_{com}$ on the ground. $\boldsymbol{m}_{os}$ is calculated by using $\boldsymbol{b}_{os}$ and $\boldsymbol{x}'_{com}$.

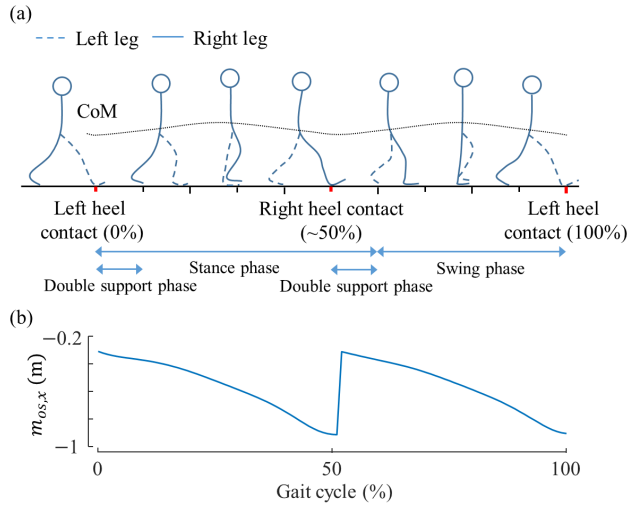

Fig. 2. Gait cycle and minimum MoS value. (a) Gait cycle (defined from the left-heel contact (0%) to the next left-heel contact (100%)) normalized to 0–100%. Modified from [17]. (b) Example of the variation in MoS along the y-axis ($m_{os,x}$) with the gait cycle.

unless a new leading foot is grounded [15], [16]. The position vector and velocity vector of CoM at a certain instant are represented as $\boldsymbol{c}_{om}$ and $\boldsymbol{v}_{com}$, respectively. $\boldsymbol{x}_{com}$ is computed by using the natural frequency of the inverted pendulum ω as

$$\boldsymbol{x}_{com} = \boldsymbol{c}_{om} + \frac{\boldsymbol{v}_{com}}{\omega} \tag{1}$$

Here, ω is calculated as

$$\omega = \sqrt{\frac{g}{l}} \tag{2}$$

where g is the acceleration of gravity, and l is the height of the CoM at an upstanding posture. MoS ($\boldsymbol{m}_{os}$) is computed by using the coordinate vector of the end of the BoS ($\boldsymbol{b}_{os}$) and $\boldsymbol{x}'_{com}$, which is the projection of $\boldsymbol{x}_{com}$ on the ground as

$$\boldsymbol{m}_{os} = \boldsymbol{b}_{os} - \boldsymbol{x}'_{com}. \tag{3}$$

We deal with the MoS in the forward direction (y-axis) and use the minimum MoS value during a gait cycle that is observed just before heel contact, as shown in Fig. 2.

III. Data from Gait Motion Database

In this study, we analyzed a subset of the gait motion database [14]. This subset included ten adult participants (age: 67.8 ± 2.5 (mean and standard deviation) years, height: 160.1 ± 8.1 cm, weight: 59.3 ± 7.7 kg) without any neurological and musculoskeletal abnormalities. They walked on a 10-meter straight course at their comfortable gait speeds. The motions of their whole body were recorded by using an optical motion capture system. The details of measurement are provided in [14].

We analyzed 53 gait trials; a trial is defined as a gait cycle from left-heel contact to the next left-heel contact while walking. The gait cycle was normalized to 0–100% for aligning the data length of each trial (Fig. 2 (a)). We analyzed the velocities of the CoM in the three-axial directions by using the x- and z-axes as well as the y-axis, which is the medio-lateral direction (left for positive) in the reference coordinate system. These CoM velocities were obtained by differentiating the position of the CoM of the whole body. Fig. 2 (b) represents the variation in MoS along the y-axis along a gait cycle.

IV. Computation of Kinematic Gait Stability Index

By using kinematic or motion data, we constructed the gait stability index that is highly correlated with the margin of stability. For this, we used PLS, which is a kind of multivariate analysis [13]. PLS determines a quantity through a linear combination of the explanatory variables. The correlation coefficient between the quantity and an objective variable is maximized. There exist multiple such quantities that are independent of each other. We applied PLS on the analysis of principal motions [17], [18], for which the explanatory variables were the multivariate time-series. In the present study, the time-series of the three-axial velocity of the center of human body were the explanatory variables. Then, multiple principal motions that are highly correlated with the minimum MoS values were determined.

For the direction j ($j = x, y, z$) at the k-th trial ($k = 1, ..., k'$), $\boldsymbol{v}_{com,j,k}$ was the time-series vector of the velocities of $\boldsymbol{c}_{om}$, comprising discretized 101 moments (one value every percent of gait cycle):

$$\boldsymbol{v}_{com,j,k} = (v_{com,j,k,1}, v_{com,j,k,2}, ..., v_{com,j,k,101}). \tag{4}$$

k' is the number of gait samples and $k' = 53$ in the present study. By using this, we constructed an extended column vector $\boldsymbol{a}_k$ ($\in \mathbb{R}^{303\times1}$) as

$$\boldsymbol{a}_k = (\boldsymbol{v}_{com,x,k}, \boldsymbol{v}_{com,y,k}, \boldsymbol{v}_{com,z,k})^{\mathrm{T}}. \tag{5}$$

The time-series data of all the motions are represented by the matrix $\boldsymbol{A}_{obs}$ ($\in \mathbb{R}^{k'\times303}$) as follows:

$$\boldsymbol{A}_{obs} = (\boldsymbol{a}_1, ..., \boldsymbol{a}_k, ..., \boldsymbol{a}_{k'})^{\mathrm{T}}. \tag{6}$$

TABLE I

CORRELATION COEFFICIENTS BETWEEN $\boldsymbol{m}_{os,min}$ AND PRINCIPAL MOTION SCORES.

First principal motion	0.71
Second principal motion	0.36
Third principal motion	0.19

In the following procedure, the main formulas of the PLS are as follows:

$$\boldsymbol{A}_{obs} = \sum_{i=1}^{n} \boldsymbol{t}_i \boldsymbol{p}_i^{\mathrm{T}} + \boldsymbol{E}_A \tag{7}$$

$$\boldsymbol{m}_{os,min} = \sum_{i=1}^{n} q_i \boldsymbol{t}_i + \boldsymbol{e}_b \tag{8}$$

Here, $\boldsymbol{m}_{os,min}$ ($\in \mathbb{R}^{k' \times 1}$) represents the vector of the minimum MoS values obtained from each trial. n is the number of principal motions, $\boldsymbol{t}_i$ ($\in \mathbb{R}^{k' \times 1}$) is the score vector for the i-th principal motion, $\boldsymbol{p}_i$ ($\in \mathbb{R}^{303 \times 1}$) is the loading of the i-th principal motion, and q_i is the regression coefficient for the i-th principal motion. $\boldsymbol{E}_A$ and $\boldsymbol{e}_b$ are the residuals of $\boldsymbol{A}$ and $\boldsymbol{m}_{os,min}$, respectively. Based on these formulas, first, $\boldsymbol{t}_1$ was determined by making the covariance of $\boldsymbol{t}_1$ and $\boldsymbol{m}_{os,min}$ the largest. $\boldsymbol{p}_1$ and q_1 are then computed to minimize the residuals in (7) and (8). $\boldsymbol{t}_2$ was then determined by making the covariance of $\boldsymbol{t}_2$ and $\boldsymbol{m}_{os,min} - q_1 \boldsymbol{t}_1$ the largest. Similarly for the third, fourth, and other principal motions. Next, the loading and coefficient of each principal motion were calculated. After adopting the appropriate number of principal motions, the objective variable was estimated as follow:

$$\bar{\boldsymbol{m}}_{os,min} = \sum_{i=1}^{n} q_i \boldsymbol{t}_i. \tag{9}$$

V. RESULT

Table I lists the correlation coefficients between $\boldsymbol{m}_{os,min}$ and the principal motion scores. Based on the magnitude of the correlation coefficients, we included up to the third principal motions in our analysis. Strong to moderate, i.e., 0.71–0.19, linear relationships were observed between the scores and the minimum MoS. The kinematic gait stability index was computed by the linear synthesis of these three principal motions:

$$\bar{\boldsymbol{m}}_{os,min} = 0.10\boldsymbol{t}_1 + 0.05\boldsymbol{t}_2 + 0.03\boldsymbol{t}_3. \tag{10}$$

Fig. 3 shows the scatter plot of $\boldsymbol{m}_{os,min}$ and $\bar{\boldsymbol{m}}_{os,min}$. Their correlation coefficient was as high as 0.82. The constructed index is highly correlated with the minimum value of MoS, unlike previous stability indices.

VI. DISCUSSION

As aforementioned, the newly constructed kinematic index exhibited concurrent validity in terms of the correlation with the minimum MoS values. The semantic validity of the index is also important. Here, we interpret the meanings

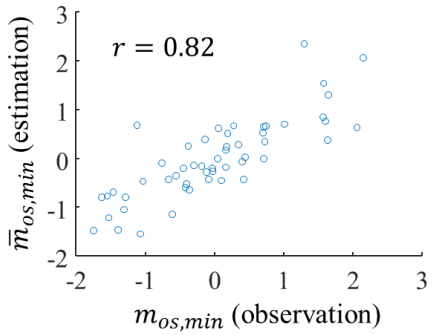

Fig. 3. Correlation between $\boldsymbol{m}_{os,min}$ and $\bar{\boldsymbol{m}}_{os,min}$.

of the principal motions by inspecting their time-series characteristics. Fig. 4 shows the time-series change for the load of the first–third principal motions. As the motion is normalized, when the load is positive, the velocity of the CoM is larger than the mean value of all trials at a certain instant.

The top of Fig. 4, which is the first principal motion, shows that the velocity of the CoM along the y-axis shifted toward the stance leg from before heel contact to the first half of the stance phase, indicating a relatively larger lateral motion. Along the y-axis, the CoM velocity tends to be slow (negative), especially during the double support phase (0–10%, 50–60% of gait cycle). Thus, the first principal motion is a characteristic motion of slow walking in the double stance phase. In other words, the slower the motion during the double-support phase, the greater the minimum MoS, and the gait is judged to be more stable. Just before the double support phase, the velocity along the y-axis is large, and the support base is small. Therefore, XCoM moves considerably ahead of BoS, making the walking motion unstable, and the MoS value is usually minimum during this phase. Therefore, it is reasonably speculated that the gait becomes more stable by employing these strategies.

The middle of Fig. 4, which is the second principal motion, represents that the CoM motion along the x-axis is opposite to the normal CoM motion because the velocity of the CoM tends to be toward the swing leg from before heel contact to the first half of the stance phase. The y-axial velocity is large (positive) during the single support phase, which is opposite to the normal motion of the CoM. In contrast, the motion of the CoM along the z-axis is the enhancement of its typical motion as it exhibits the maximum value at toe off and the minimum value at heel contact. Collectively, the second principal motion represents walking motion with a small change in the velocity of the CoM along the x- and y-axes.

The bottom of Fig. 4, which is the third principal motion, indicates that the velocity of the CoM along the x-axis is similar to the reversal of the first principal motion. The velocity of the CoM along the y-axis is slow (negative). The velocity of the CoM along the z-axis is large (positive) in the single support phase, and it is maximum before heel

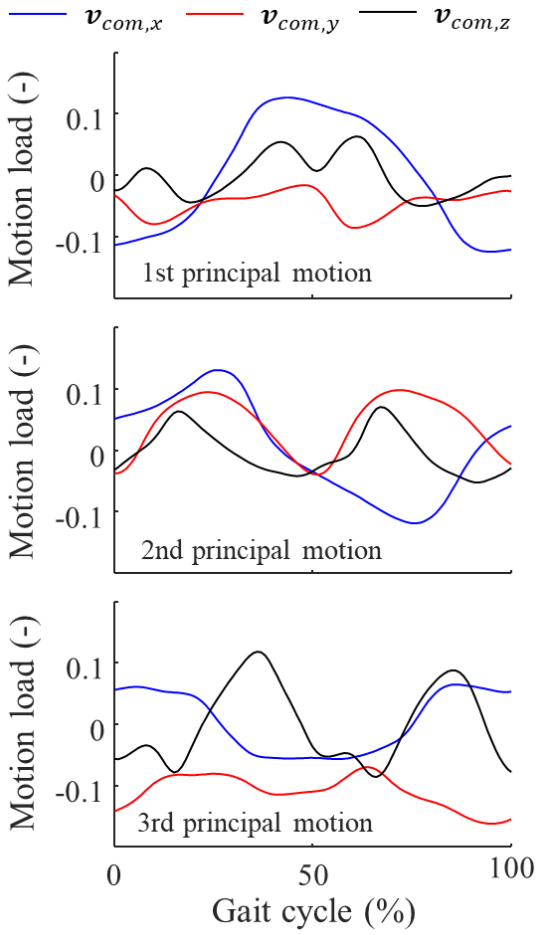

Fig. 4. Substance each principal motion. Top: first principal motion. Middle: second principal motion. Bottom: third principal motion. A positive load at an instant indicates that the velocity is greater than the average velocities among all trials.

contact. From these characteristics, the third principal motion may be related to the small step length. In fact, Pai and Patton [16] demonstrated that a decrease in the step length, for an unchanged walking speed, led to an increase in MoS in the backward direction.

VII. CONCLUSION

We constructed a new kinematic gait stability index that is highly correlated with a popular kinetic stability index i.e., the MoS. This index uses the velocity of the center of the human body and is designed to be correlated with the MoS by using a method of principal motion analysis. Unlike previous kinematic indices, this index exhibited a high correlation coefficient of 0.82 with the MoS. This suggests that the index can be used as an easy-to-measure alternative of the MoS. In this study, the MoS was computed by using the velocities of the CoM measured by a camera-based motion capture system, but the same results can be expected by using IMU.

Although we analyzed the data of ten participants in the present study, the gait motion database we used originally included more participants, and a greater number of participants should be analyzed in the future. Our approach will be applied along the medio-lateral direction as well as the frontal-back direction. Finally, the general applicability of the index should be tested via cross-validation.

REFERENCES

[1] S. A. England and K. P. Granata, "The influence of gait speed on local dynamic stability of walking," *Gait & Posture*, vol. 25, no. 2, pp. 172–178, 2007.

[2] S. M. Bruijn, J. H. van Dieen, O. G. Meijer, and P. J. Beek, "Is slow walking more stable?" *Journal of Biomechanics*, vol. 42, no. 10, pp. 1506–1512, 2009.

[3] T. M. Owings and M. D. Grabiner, "Variability of step kinematics in young and older adults," *Gait & Posture*, vol. 20, no. 1, pp. 26–29, 2004.

[4] L. Hak, H. Houdijk, P. J. Beek, and J. H. van Dieën, "Steps to take to enhance gait stability: the effect of stride frequency, stride length, and walking speed on local dynamic stability and margins of stability," *Plos One*, vol. 8, no. 12, 2013.

[5] Y. Akiyama, Y. Fukui, S. Okamoto, and Y. Yamada, "Effects of exoskeletal gait assistance on the recovery motion following tripping," *Plos One*, vol. 15, no. 2, p. e0229150, 2020.

[6] Y. Akiyama, K. Mitsuoka, S. Okamoto, and Y. Yamada, "Experimental analysis of the fall mitigation motion caused by tripping based on the motion observation until shortly before ground contact," *Journal of Biomechanical Science and Engineering*, vol. 14, no. 1, pp. 18–00 510, 2019.

[7] S. Bruijn, O. Meijer, P. Beek, and J. v an Dieen, "Assessing the stability of human locomotion: a review of current measures," *Journal of the Royal Society Interface*, vol. 10, no. 83, p. 20120999, 2013.

[8] A. Hof, M. Gazendam, and W. Sinke, "The condition for dynamic stability," *Journal of Biomechanics*, vol. 38, no. 1, pp. 1–8, 2005.

[9] J. B. Dingwell and J. P. Cusumano, "Nonlinear time series analysis of normal and pathological human walking," *Interdisciplinary Journal of Nonlinear Science*, vol. 10, no. 4, pp. 848–863, 2000.

[10] L. Hak, H. Houdijk, F. Steenbrink, A. Mert, P. van der Wurff, P. J. Beek, and J. H. van Dieën, "Speeding up or slowing down?: Gait adaptations to preserve gait stability in response to balance perturbations," *Gait & posture*, vol. 36, no. 2, pp. 260–264, 2012.

[11] M. F. Vieira, G. S. d. S. e Souza, G. C. Lehnen, F. B. Rodrigues, and A. O. Andrade, "Effects of general fatigue induced by incremental maximal exercise test on gait stability and variability of healthy young subjects," *Journal of Electromyography and Kinesiology*, vol. 30, pp. 161–167, 2016.

[12] F. Yang and Y.-C. Pai, "Can stability really predict an impending slip-related fall among older adults?" *Journal of Biomechanics*, vol. 47, no. 16, pp. 3876–3881, 2014.

[13] S. Wold, M. Sjöström, and L. Eriksson, "PLS-regression: a basic tool of chemometrics," *Chemometrics and Intelligent Laboratory Systems*, vol. 58, no. 2, pp. 109–130, 2001.

[14] Y. Kobayashi, N. Hida, K. Nakajima, M. Fujimoto, and M. Mochimaru, "2019: Aist gait database," 2019.

[15] D. D. Espy, F. Yang, T. Bhatt, and Y.-C. Pai, "Independent influence of gait speed and step length on stability and fall risk," *Gait & Posture*, vol. 32, no. 3, pp. 378–382, 2010.

[16] Y.-C. Pai and J. Patton, "Center of mass velocity-position predictions for balance control," *Journal of Biomechanics*, vol. 30, no. 4, pp. 347–354, 1997.

[17] T. Iwasaki, S. Okamoto, Y. Akiyama, and Y. Yamada, "Principal motion ellipsoids: Gait variability index based on principal motion analysis," in *Proceedings of IEEE/SICE International Symposium on System Integration*, 2020, pp. 489–494.

[18] ——, "Generalized principal motion analysis: classification of sit-to-stand motions," in *Proceedings of IEEE Global Conference on Consumer Electronics*, 2019, pp. 679–681.